EXTENDED PDF FORMAT
SPONSORED BY
www.usbweb.com

Self-Repairing Oxetane-Substituted Chitosan Polyurethane Networks

Biswajit Ghosh, *et al.*

Science **323**, 1458 (2009);
DOI: 10.1126/science.1167391

The following resources related to this article are available online at www.sciencemag.org (this information is current as of March 21, 2009):

Updated information and services, including high-resolution figures, can be found in the online version of this article at:
http://www.sciencemag.org/cgi/content/full/323/5920/1458

Supporting Online Material can be found at:
http://www.sciencemag.org/cgi/content/full/323/5920/1458/DC1

A list of selected additional articles on the Science Web sites **related to this article** can be found at:

http://www.sciencemag.org/cgi/content/full/323/5920/1458#related-content

This article **cites 21 articles**, 2 of which can be accessed for free:
http://www.sciencemag.org/cgi/content/full/323/5920/1458#otherarticles

This article appears in the following **subject collections**:
Chemistry
http://www.sciencemag.org/cgi/collection/chemistry

Information about obtaining **reprints** of this article or about obtaining **permission to reproduce this article** in whole or in part can be found at:
http://www.sciencemag.org/about/permissions.dtl

Downloaded from www.sciencemag.org on March 21, 2009

Science (print ISSN 0036-8075; online ISSN 1095-9203) is published weekly, except the last week in December, by the American Association for the Advancement of Science, 1200 New York Avenue NW, Washington, DC 20005. Copyright 2009 by the American Association for the Advancement of Science; all rights reserved. The title *Science* is a registered trademark of AAAS.

the formation of prenucleation clusters with dimensions of 0.6 to 1.1 nm (step 0). In analogy to the chemistry of calcium phosphate (*31*), we consider them to be the smallest stable agglomerates of CaCO$_3$ present from the beginning of the reaction. Aggregation of these clusters in solution leads to the nucleation of ACC nanoparticles with a size distribution centered around 30 nm (step 1). Association of these particles with the template surface initiates the growth of ACC (step 2), using the nanoparticles in their neighborhood as feedstock. Next, randomly oriented nanocrystalline domains are formed inside the otherwise amorphous particles (steps 3 and 4). On the basis of the model of Zhang *et al.* (*23*), we expect these domains to be unstable and in equilibrium with the amorphous phase. In the last steps, the orientation that is stabilized through the interaction with the monolayer becomes dominant (step 5) and develops into a single crystal (step 6). This single crystal probably grows by the further addition and incorporation of ions and clusters from solution.

The initial experiments of Mann and co-workers showed that the present system could produce calcite (1$\bar{1}$.0) or vaterite (00.1) depending on the precise conditions (*16*, *32*). Later, it was demonstrated that rapid CO$_2$ evaporation favors the kinetic product, vaterite (*21*, *22*), whereas lower evaporation rates lead to the calcitic form (*21*). These results are confirmed by our finding of (00.1) oriented vaterite in the present work (i.e., in a fast-outgassing thin film) and the formation of (1$\bar{1}$.0) oriented calcite in crystallization dishes (fig. S7) (*15*) from which CO$_2$ outgassing is slower. Moreover, the observation of randomly oriented vaterite crystals also puts in perspective the synchrotron x-ray scattering experiments that showed the formation of randomly oriented crystals from the same system (*22*).

The nanoscopic prenucleation clusters that we visualized are the smallest stable form of CaCO$_3$ and are likely the building blocks of the amorphous precursor particles observed in biomineralization; such particles are also observed in many synthetic systems and are not restricted to calcium carbonate (*13*, *31*). As a consequence of their aggregation, ACC nucleates in solution and subsequently assembles at the template. There, it is present as a temporarily stabilized but transient phase that mediates the transfer of information from the template to the mineral phase. This occurs through the selective stabilization of only one of the orientations present, leading to the development of a single crystal.

References and Notes

1. H. A. Lowenstam, S. Weiner, *On Biomineralization* (Oxford Univ. Press, New York, 1989).
2. M. E. Davis, *Science* **305**, 480 (2004).
3. B. L. Smith *et al.*, *Nature* **399**, 761 (1999).
4. J. Aizenberg *et al.*, *Science* **309**, 275 (2005).
5. J. R. Young, J. M. Didimus, P. R. Bown, B. Prins, S. Mann, *Nature* **356**, 516 (1992).
6. L. Addadi, D. Joester, F. Nudelman, S. Weiner, *Chem. Eur. J.* **12**, 980 (2006).
7. N. A. J. M. Sommerdijk, G. de With, *Chem. Rev.* **108**, 4499 (2008).
8. M. Volmer, *Kinetik der Phasenbildung* (Steinkopff, Dresden, 1939).
9. Y. Politi, T. Arad, E. Klein, S. Weiner, L. Addadi, *Science* **306**, 1161 (2004).
10. E. Beniash, J. Aizenberg, L. Addadi, S. Weiner, *Proc. R. Soc. London Ser. B* **264**, 461 (1997).
11. B. P. Pichon, P. H. H. Bomans, P. M. Frederik, N. A. J. M. Sommerdijk, *J. Am. Chem. Soc.* **130**, 4034 (2008).
12. J. R. I. Lee *et al.*, *J. Am. Chem. Soc.* **129**, 10370 (2007).
13. D. Gebauer, A. Völkel, H. Cölfen, *Science* **322**, 1819 (2008).
14. C. L. Freeman, J. H. Harding, D. M. Duffy, *Langmuir* **24**, 9607 (2008).
15. See supporting material on *Science* Online.
16. S. Mann, B. R. Heywood, S. Rajam, J. D. Birchall, *Nature* **334**, 692 (1988).
17. S. Nickell, C. Kofler, A. P. Leis, W. Baumeister, *Nat. Rev. Mol. Cell Biol.* **7**, 225 (2006).
18. The sedimentation coefficient s is defined as the velocity v_t of the particle per unit gravitational acceleration (centrifugal acceleration: $\omega^2 r$, where ω is angular velocity and r is the radial distance to the rotation axis).
19. F. M. Michel *et al.*, *Chem. Mater.* **20**, 4720 (2008).
20. D. Quigley, P. M. Rodger, *J. Chem. Phys.* **128**, 221101 (2008).
21. E. Loste, E. Diaz-Marti, A. Zarbakhsh, F. C. Meldrum, *Langmuir* **19**, 2830 (2003).
22. E. DiMasi, M. J. Olszta, V. M. Patel, L. B. Gower, *CrystEngComm* **5**, 346 (2003).
23. T. H. Zhang, X. Y. Liu, *J. Am. Chem. Soc.* **129**, 13520 (2007).
24. Y. Politi *et al.*, *Adv. Funct. Mater.* **16**, 1289 (2006).
25. R. S. K. Lam, J. M. Charnock, A. Lennie, F. C. Meldrum, *CrystEngComm* **9**, 1226 (2007).
26. J. Aizenberg, D. A. Muller, J. L. Grazul, D. R. Hamann, *Science* **299**, 1205 (2003).
27. R. Tang *et al.*, *Angew. Chem. Int. Ed.* **43**, 2697 (2004).
28. G. Luquet, F. Marin, *C. R. Palevol* **3**, 515 (2004).
29. L. Brecevic, A. E. Nielsen, *J. Cryst. Growth* **98**, 504 (1989).
30. J. J. J. M. Donners, B. R. Heywood, E. W. Meijer, R. J. M. Nolte, N. A. J. M. Sommerdijk, *Chem. Eur. J.* **8**, 2561 (2002).
31. A. S. Posner, F. Betts, *Acc. Chem. Res.* **8**, 273 (1975).
32. S. Rajam *et al.*, *J. Chem. Soc. Faraday Trans.* **87**, 727 (1991).
33. Supported by the European Community (project code NMP4-CT-2006-033277) and the Netherlands Organization for Scientific Research (NWO). We thank A. Völkel and H. Cölfen for performing and evaluating the ultracentrifugation measurements; D. Gebauer and A. Verch for time-dependent solution composition determination of the mineralization solutions; F. L. Boogaard, E. J. Creusen, J. J. van Roosmalen, and P. Moeskops for their contribution to the 3D reconstructions of the tomograms; and P. T. K. Chin for providing the CdSe nanorods.

Supporting Online Material
www.sciencemag.org/cgi/content/full/323/5920/1455/DC1
Materials and Methods
SOM Text
Table S1
Figs. S1 to S7

5 December 2008; accepted 30 January 2009
10.1126/science.1169434

Self-Repairing Oxetane-Substituted Chitosan Polyurethane Networks

Biswajit Ghosh and Marek W. Urban*

Polyurethanes have many properties that qualify them as high-performance polymeric materials, but they still suffer from mechanical damage. We report the development of polyurethane networks that exhibit self-repairing characteristics upon exposure to ultraviolet light. The network consists of an oxetane-substituted chitosan precursor incorporated into a two-component polyurethane. Upon mechanical damage of the network, four-member oxetane rings open to create two reactive ends. When exposed to ultraviolet light, chitosan chain scission occurs, which forms crosslinks with the reactive oxetane ends, thus repairing the network. These materials are capable of repairing themselves in less than an hour and can be used in many coatings applications, ranging from transportation to packaging or fashion and biomedical industries.

When a hard or sharp object hits a vehicle, it is likely that it will leave a scratch, and for this reason the automotive industry looks for coatings with high scratch resistance. Because of their hardness and elasticity, polyurethanes exhibit good scratch resistance but can still suffer from mechanical damage. An ideal automotive coating would mend itself while a vehicle is driven. To heal mechanical damage in plants, suberin, tannins, phenols, or nitric oxide are activated to prevent further lesions (*1*–*3*), whereas in a human skin, the outer flow of blood cells is arrested by the crosslink network of fibrin, giving rise to wound-healing (*4*, *5*). Concentration gradients or stratification in living organisms inspired the development of spatially heterogeneous remendable polymers (*6*, *7*), composites containing micro-encapsulated spheres (*8*–*11*), encapsulated fibers (*12*–*14*), reversible cross-linking (*15*, *16*), and microvascular networks (*17*). One example is epoxy matrices containing a glass hollow fiber filled with a monomer and an initiator with the "bleeding" ability to heal polymer networks during crack formation (*12*). A similar phenomenon was used in another approach, in which a micro-encapsulated dicyclopentadiene monomer was introduced in a catalyst-embedded polymer matrix, which healed the crack near the ring opening of the monomer (*8*–*11*). Reversibility of Diels-Alder reactions resulted in another approach to thermally repair damaged areas, and approach using malemide-furan adducts (*15*, *16*). Mimicking of microvascular structures (*17*), water-responsive expandable gels (*7*), and formation of supramolecular assemblies (*18*) are other avenues of remendability.

This study departs from previous approaches and reports the development of heterogeneous

---

School of Polymers and High Performance Materials, Shelby F. Thames Polymer Science Research Center, The University of Southern Mississippi, Hattiesburg, MS 39406, USA.

*To whom correspondence should be addressed. E-mail: marek.urban@usm.edu

polyurethane (PUR) networks based on oxetane-substituted derivative of chitosan (OXE-CHI), which upon reaction with hexamethylene diisocyante (HDI) and polyethylene glycol (PEG) (*19*) form heterogeneous OXE-CHI-PUR networks. The choice of these components was driven by their ability to serve specific functions; PUR networks provide desirable heterogeneity through polyurethane and polyurea components, and OXE-CHI provides the cleavage of a constrained four-membered ring (OXE) and ultraviolet (UV) sensitivity through CHI, the latter being a product of deacetylation of chitin, which is the structural element of exoskeletons of crustaceans (e.g., crabs and shrimp) occurring in abundance in nature. Figure 1 illustrates a two-step reaction sequence leading to the OXE-CHI-PUR formation (*20*). The first step in this investigation was the synthesis of OXE-CHI, in which the primary alcohol of CHI was reacted with chloromethyl of OXE (*21*). An OXE ring was reacted to the C_6 position of the chitosan molecule, which is confirmed by infrared (IR), Raman, and ^{13}C-NMR (nuclear magnetic resonance) spectroscopy (*20*) (figs. S1, S2, and S3, respectively). The second step illustrates the reactions leading to the incorporation of OXE-CHI into trifunctional HDI in the presence of PEG (1:1.4 and 1:1.33 molar ratios), confirmed by IR and ^{13}C-NMR spectroscopy (*20*) (figs. S4 and S5, respectively).

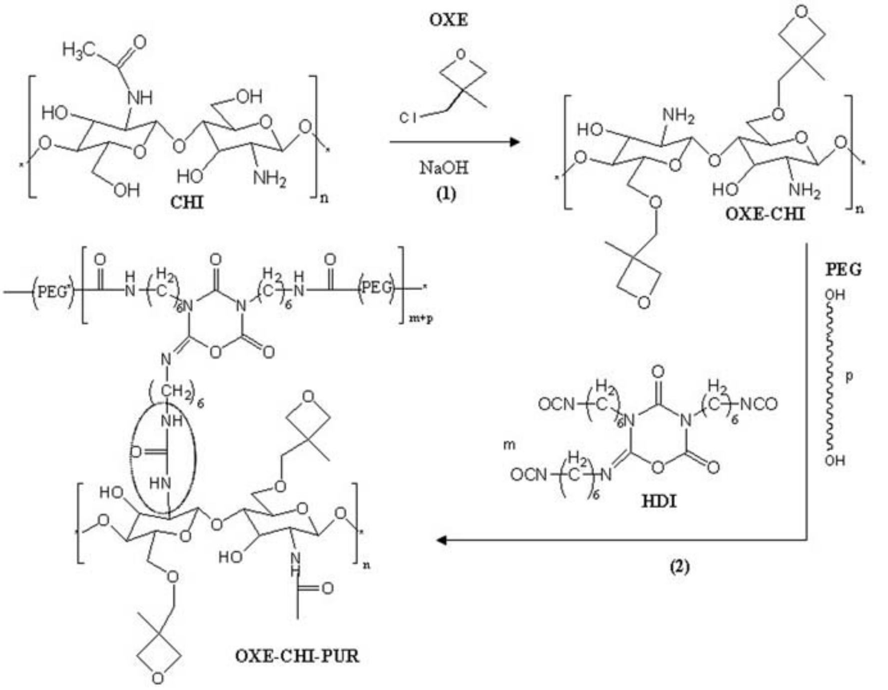

Fig. 1. Synthetic steps involved in the formation of OXE-CHI. 1, Reactions of OXE with CHI, leading to the formation of OXE-CHI precursor; 2, Reactions of OXE-CHI with HDI and PEG, leading to formations of remendable OXE-CHI-PUR network.

Networks were allowed to crosslink under ambient conditions to form solid films and then were mechanically damaged by creating a scratch. Figure 2A1 illustrates a mechanical damage of OXE-CHI-PUR films. When the damaged area is exposed to a 120 W fluorescent UV lamp at 302 nm wavelength of light for 15 (Fig. 2A2) and 30 (Fig. 2A3) min, the damaged area vanishes. The upper portion of Fig. 2 illustrates IR images of the damaged area, whereas the lower part illustrates optical images. Also, IR images of the damaged area exhibit chemical changes resulting from the repair and are shown in figs. S8 and S9. A series of controlled experiments were conducted on specimens prepared by varying molar ratios of OXE-CHI with respect to the PUR content (table S1). Optical images shown in Fig. 3, A to D, illustrate the results of the experiments conducted under the same UV exposure conditions (0, 15, and 30 min) conducted on the specimens listed in table S1.

These experiments illustrate that the presence of OXE-CHI precursor is the key factor responsible for remendability of the network (Figs. 2 and 3). Neither PUR nor CHI-PUR alone (table S1, specimens A and B) is able to repair the mechanical damage, whereas the presence of covalently bonded OXE-CHI (table S1, specimens C and D) entities facilitates the self-healing process.

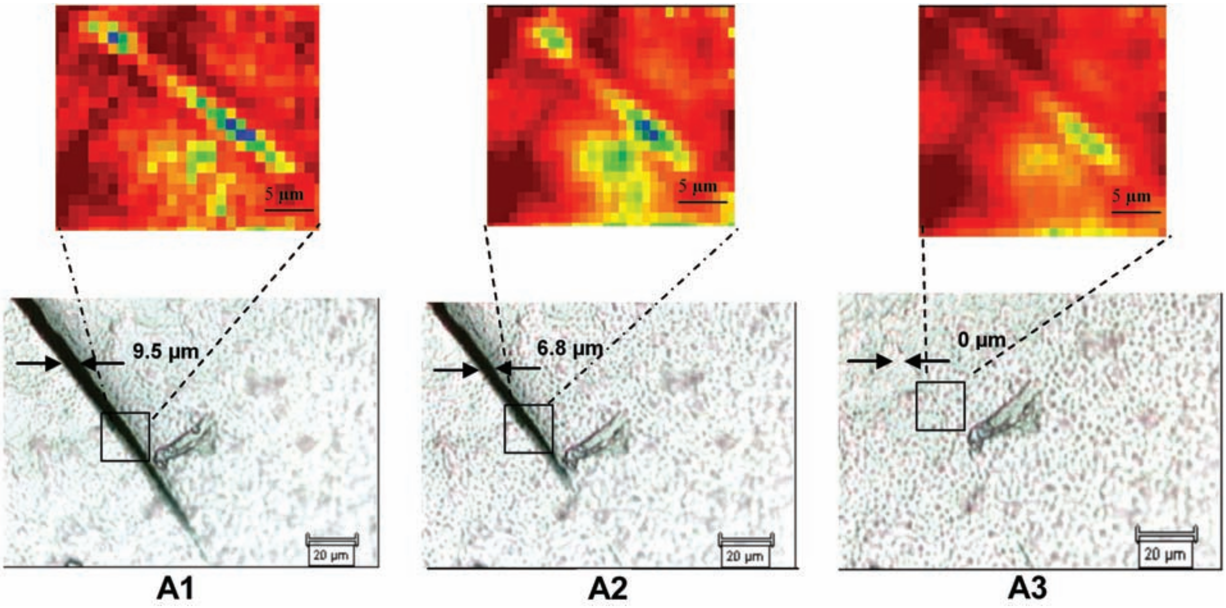

Fig. 2. IR (**upper**) and optical (**lower**) images of OXE-CHI-PUR networks recorded as a UV exposure time. A1, 0 min; A2, 15 min; A3, 30 min. (SOM provides details regarding spectroscopic changes detected by IR imaging.)

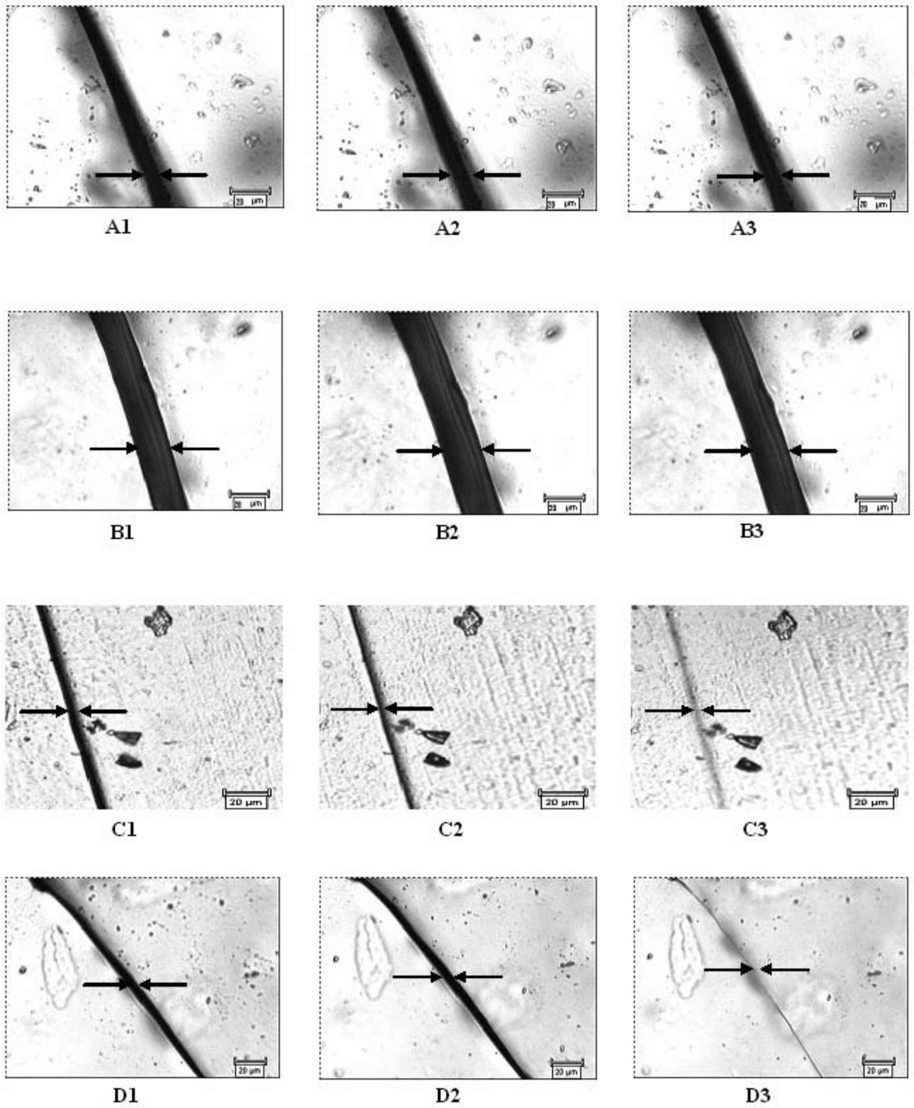

Fig. 3. Optical images of mechanically damaged films: PUR (A1, A2, and A3 are images after exposure for 0, 15, and 30 min to UV radiation; HDI/PEG/CHI = 1:1.5:0); CHI-PUR (B1, B2, and B3 are images after exposure for 0, 15, and 30 min to UV radiation; HDI/PEG/CHI = 1:1.4:0.57 × 10^{-4}); OXE-CHI-PUR (C1, C2, and C3 are images after exposure for 0, 15, and 30 min to UV radiation; HDI/PEG/OXE-CHI = 1:1.4:0.57 × 10^{-4}); OXE-CHI-PUR (D1, D2, and D3 are images after exposure for 0, 15, and 30 min to UV radiation; HDI/PEG/OXE-CHI = 1:1.33:1.17 × 10^{-4}).

Table S1 also shows the damage width as a function of UV exposure evaluations conducted on the specimens shown in Fig. 3. The rate of repair for networks containing half the OXE-CHI precursor concentration is also reduced.

Although a cut is a local event at micrometer or smaller scales, the actual cleavage is a molecular-level event. To determine the mechanism of repair and to follow molecular events in the damaged area, we used localized micro-attenuated total reflectance (ATR) Fourier transform IR (FTIR) spectroscopy (*22*) and internal reflection IR imaging (IRIRI) (*23*). As shown in figs. S6 and S7, the loss of urea and ether linkages of CHI (circled in Fig. 1) containing OXE rings results from the UV light exposure of damaged surface areas responsible for repairing. In these experiments, the repair process uses UV light to recombine free radicals to form crosslinks. In the 280 to 400 nm range, a fluorescent UV lamp generates approximately 0.3 W/m^2 per nm power density, whereas the Sun gives off about 0.25 W/m^2 per nm (*24*). Thus, the time frames for repair of the Sun exposure are very similar, although the energy density changes as a function of the wavelength of radiation for both sources vary somewhat. As a result of stronger Sun radiation during the summer months in the southern United States, the repair process will be about 3 to 4 times as fast compared with the equivalent exposure in the northern United States, but for the winter months this difference will be negligible (*25*). Because crosslinking reactions are not moisture sensitive, dry or humid climate conditions will not affect the repair process. The above networks exhibit the ability to self-repair upon exposure to UV light, but if exactly the same previously repaired spot is damaged again, the ability for further repair may be limited by the thermosetting characteristics of these networks.

We developed a new generation of thermosetting polymers that are of considerable technical and commercial importance. The use of the UV portion of the electromagnetic radiation for repairing mechanical damages in coatings offers an ambient temperature approach to self-healing—critical in a number of applications and technologies that do not require the placement of other, often elaborate, network components—that is controlled by the chemistries and morphologies of polymer networks.

References and Notes

1. J. Leon, E. Rojo, J. J. Sanchez-Serrano, *J. Exp. Bot.* **52**, 1 (2001).
2. R. F. Diegelmann, M. C. Evans, *Front. Biosci.* **9**, 283 (2004).
3. R. Paris, L. Lamattina, C. A. Casalongue, *Plant Physiol. Biochem.* **45**, 80 (2007).
4. G. Henry, W. Li, W. Garner, D. T. Woodley, *Lancet* **361**, 574 (2003).
5. K. G. Mann, K. Brummel-Ziedins, T. Orefo, S. Butenas, *Blood Cells Mol. Dis.* **36**, 108 (2006).
6. P. Sonntag *et al.*, *Nat. Mater.* **3**, 311 (2004).
7. K. Nagaya, S. Ikai, M. Chiba, X. Chao, *JSME Int. J. Ser. C* **49**, 379 (2006).
8. S. R. White *et al.*, *Nature* **409**, 794 (2001).
9. E. N. Brown, M. R. Kessler, N. R. Sottos, S. R. White, *J. Microencapsul.* **20**, 719 (2003).
10. E. N. Brown, S. R. White, N. R. Sottos, *J. Mater. Sci.* **39**, 1703 (2004).
11. M. R. Kessler, N. R. Sottos, S. R. White, *Composites Part A* **34**, 743 (2003).
12. J. W. C. Pang, I. P. Bond, *Compos. Sci. Technol.* **65**, 1791 (2005).
13. J. W. C. Pang, I. P. Bond, *Composites Part A* **36**, 183 (2005).
14. S. R. Trask, H. R. Williams, I. P. Bond, *Bioinspir. Biomim.* **2**, P1 (2007).
15. X. Chen *et al.*, *Science* **295**, 1698 (2002).
16. R. Gheneim, C. Perez-Berumen, A. Gandini, *Macromolecules* **35**, 7246 (2002).
17. S. K. Toohey, N. R. Sottos, J. A. Lewis, J. S. Moore, S. R. White, *Nat. Mater.* **6**, 581 (2007).
18. P. Cordier, F. Tournilhac, C. Soulie-Ziakovic, L. Leiber, *Nat. Lett.* **451**, 977 (2008).
19. D. B. Otts, M. W. Urban, *Polymer (Guildf.)* **46**, 2699 (2005).
20. Materials and methods and additional data are available as supporting material on *Science* Online.
21. Y. Wan, K. A. M. Creber, B. Peppley, V. T. Bui, *J. Polym. Sci. Part B Polym. Phys* **42**, 1379 (2004).
22. M. W. Urban, *Attenuated Total Reflectance Spectroscopy of Polymers; Theory and Applications* (American Chemical Society and Oxford University Press, Washington, DC, 1996)
23. D. Otts, P. Zhang, M. W. Urban, *Langmuir* **18**, 6473 (2002).
24. Average Optimum Direct Global Radiation, Miami, FL, USA; Atlas Material Testing Technology; http://www.atlas-mts.com.
25. National Oceanographic and Atmospheric Administration, 2008; http://www.cpc.ncep.noaa.gov/products/stratosphere/uv_index/gif_files/spectrum.gif (www.noaa.gov).
26. These studies were primarily supported by the National Science Foundation MRSEC under DMR 0213883 and the Materials Research Instrumentation (MRI) Program under DMR 0215873. We thank the Mississippi Division of Marine Resources for partial support.

Supporting Online Material

www.sciencemag.org/cgi/content/full/323/5920/1458/DC1
Materials and Methods
SOM Text
Figs. S1 to S10
Table S1
References

20 October 2008; accepted 29 January 2009
10.1126/science.1167391